analytical chemistry

Letter

pubs.acs.org/ac

Quantitative Characterization of Nanoparticles in Blood by Transmission Electron Microscopy with a Window-Type Microchip Nanopipet

Lin-Ai Tai,[†] Yu-Ting Kang,[‡] Yu-Ching Chen,[†] Yu-Chao Wang,[†] Yu-Jing Wang,[†] Yu-Ting Wu,[†] Kuo-Liang Liu,[‡] Chiu-Yen Wang,[‡] Yu-Feng Ko,[§] Ching-Ya Chen,[†] Nai-Chun Huang,[†] Jen-Kun Chen,[†] Yong-Fen Hsieh,[§] Tri-Rung Yew,*[,‡] and Chung-Shi Yang*[,†]

[†]Center for Nanomedicine Research, National Health Research Institutes, Zhunan, 350, Taiwan

[‡]Department of Materials Science and Engineering, National Tsing-Hua University, Hsinchu, 300, Taiwan

[§]Materials Analysis Technology Inc., Hsinchu, 300, Taiwan

Supporting Information

ABSTRACT: Transmission electron microscopy (TEM) is a unique and powerful tool for observation of nanoparticles. However, due to the uneven spatial distribution of particles conventionally dried on copper grids, TEM is rarely employed to evaluate the spatial distribution of nanoparticles in aqueous solutions. Here, we present a microchip nanopipet with a narrow chamber width for sorting nanoparticles from blood and preventing the aggregation of the particles during the drying process, enabling quantitative analysis of their aggregation/agglomeration states and the particle concentration in aqueous solutions. This microchip is adaptable to all commercial TEM holders. Such a nanopipet proves to be a simple and convenient sampling device for TEM image-based quantitative characterization.

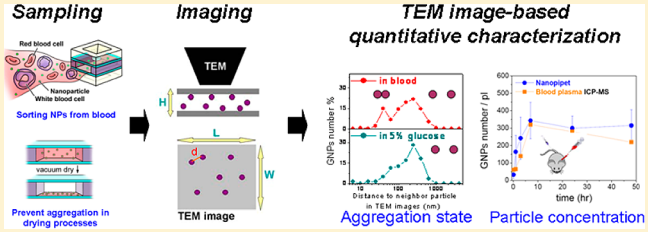

Nanoparticles or nanoparticle-based formulations offer the advantage of efficient delivery to the target tissue for enhanced therapeutic or diagnostic purposes, which is usually related to their size, shape, surface properties, and aggregation/agglomeration states.[1−6] Comprehensive physicochemical characterization of nanoparticles with respect to their size/size distribution, aggregation/agglomeration state, and shape in aqueous or physiological environments is important, yet challenging,[7,8] for their use in biomedical applications[9,10] and compliance with safety regulations.[11−14] The aggregation/agglomeration of nanoparticles in biological fluids plays a critical role in determining the physical size, shape, and surface properties that are crucial for biological recognition, yet the image-based observation of such aggregation/agglomeration is difficult to achieve. Transmission electron microscopy (TEM) is a unique and powerful tool for observation of nanoparticles.[15−18] However, due to the uneven spatial distribution of the particles conventionally dried on copper grids, TEM is rarely employed for the evaluation of the spatial distribution of nanoparticles in aqueous solutions. Here, a microchip nanopipet with a narrow chamber width was constructed to prevent the aggregation of the particles during the drying process, enabling the quantitative analysis of their aggregation/agglomeration states and particle concentration in blood (Figure 1). The upper substrate of the nanopipet breaks the surface tension of the sample droplet, suppressing the capillary flow accompanied with the evaporation of water[19] and the aggregation of the substances when the droplet is conventionally dried on a copper grid. This nanopipet acts as a prefilter for simple and convenient sorting of PEGylated gold nanoparticles[20] in whole blood, 50% diluted blood, and 5% glucose solution. The slight aggregation of carboxyl-PEG5k-modified gold nanoparticles (~18%) in a 50% diluted blood sample was observed while they were well-dispersed in a 5% glucose solution. Moreover, a consistent concentration for the cPEG5k-GNPs was obtained using the nanopipet and inductively coupled plasma-mass spectrometry (ICPMS) analysis for both in vitro 50% diluted blood and in vivo whole blood.

We examined the possibility of the use of a nanopipet to obtain the aggregation/agglomeration states of particles in aqueous solutions. Carboxyl-PEG5k-modified gold nanoparticles (cPEG5k-GNPs) (Figure 1S, Supporting Information), which are known to be long circulating and in a well-dispersed colloidal form in blood,[20] were dissolved in 5% glucose solution and used as model particles for examining and comparing the spatial distribution of the particles in TEM specimens dried in the nanopipet (with an Si_xN_y-film) and on copper grids (with either a carbon-film or an SiO_x-film). An even spatial distribution of the particles was observed in the nanopipet

Received: June 4, 2012
Accepted: July 16, 2012
Published: July 16, 2012

   dx.doi.org/10.1021/ac301523n | *Anal. Chem.* 2012, 84, 6312−6316

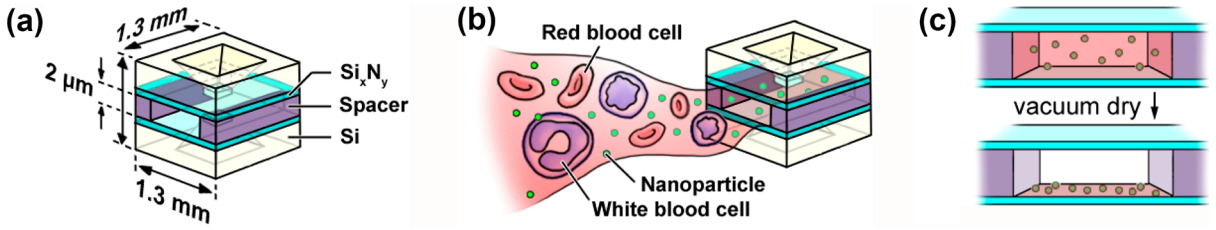

Figure 1. Geometry of the window-type TEM microchip nanopipet and sampling processes for specimen preparation: (a) schematic diagram of the device, with the dimensions and materials as indicated; (b) the nanopipet acts as a prefilter for simple and convenient sorting of nanoparticles to prevent entry of larger substances in the blood; (c) magnified schematic diagram of the chamber with a well-defined chamber width for controlling the drying processes.

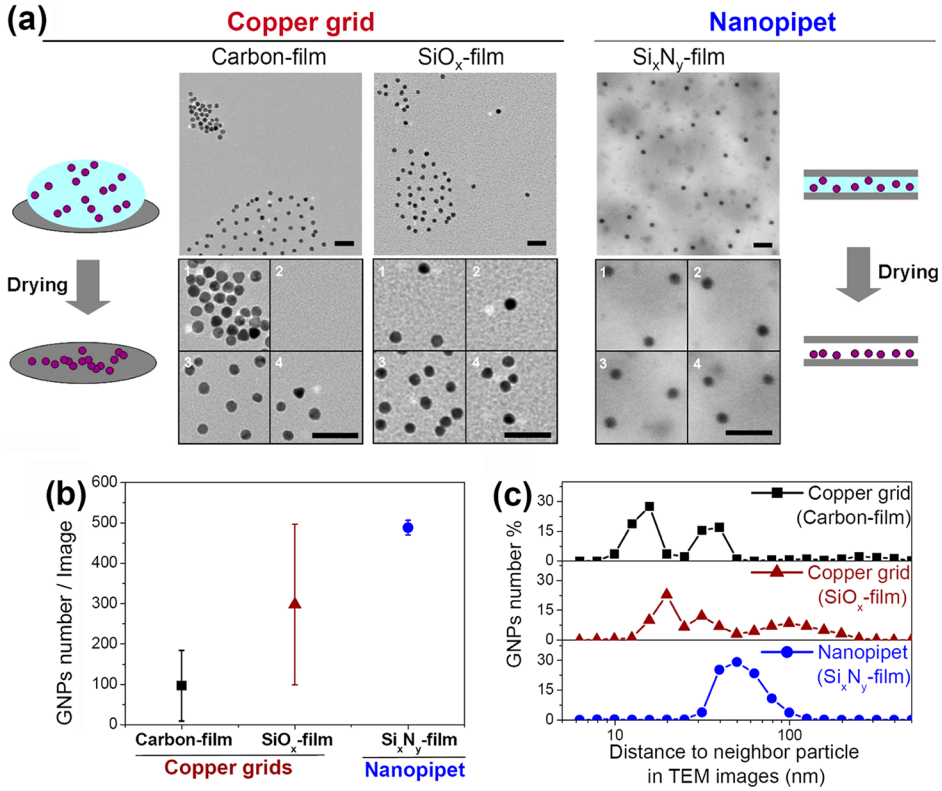

Figure 2. Drying processes and distribution of cPEG5k-GNPs on copper grids and the nanopipet: (a) TEM images of cPEG5k-GNPs in a 5% glucose solution dried on copper grids (with carbon and SiO_x films) and in the nanopipet (with an Si_xN_y-film); (b) counted particle numbers in four individual image zones (2.0 μm × 2.7 μm); (c) particle number percentage vs the distance to neighboring particles in the TEM images (sum of the four image zones). Scale bar is 50 nm.

with an Si_xN_y-film[21] (water contact angle: ~32°), with the particle number in four randomly chosen 2.0 μm × 2.7 μm image zones determined to be 478, 467, 502, and 504 (Figure 2a,b). The distance of each cPEG5k-GNP to the nearest adjacent particle (d) was also measured for all four of the 2.0 μm × 2.7 μm image zones, and the particle number percentage (n/N) was plotted versus the distance to the neighboring particle (d). A single broad distribution peak was observed with a mean distance of 69.4 ± 21.6 nm (Figure 2c), which is larger than the diameter of cPEG5k-GNP (~39.6 nm as observed by TEM, ~ 39.3 nm as measured by DLS), and indicates that most of the particles are separated from the neighboring particles. The higher percentage of particles distributed at d values greater than the particle diameter suggests that most of the particles are distributed without contact and separated without aggregation. These results are in accordance with the understanding of cPEG5k-GNPs, which are well-dispersed in 5% glucose solution, and indicate that the nanopipet can preserve the native spatial distribution of the particles and avoid aggregation/agglomeration in the sample solution. However, when the same sample solution was dried on the copper grid with a hydrophobic carbon-film[22] (water contact angle: ~70°) and even on the grid with a hydrophilic SiO_x-film[23] (water contact angle: ~30°), an obvious uneven spatial distribution of the particles was observed (Figure 2a,b). From the plot of the particle number percentage vs distance to the neighboring particle (d), three peaks were obtained for both the carbon-film and SiO_x-film copper grids (Figure 2c). The presence of two peaks with a distance smaller than the diameter of the cPEG5k-GNPs suggests that the particles are vertically stacked or self-aggregated on the copper grids during the drying process (gradual evaporation of the bulk solvent), and even the hydrophilic surface modification with an SiO_x-film cannot prevent aggregation. In another example, 300 nm polystyrene beads were dried both in nanopipets and on copper grids. The beads were well separated in the nanopipets but highly

dx.doi.org/10.1021/ac301523n | Anal. Chem. 2012, 84, 6312–6316

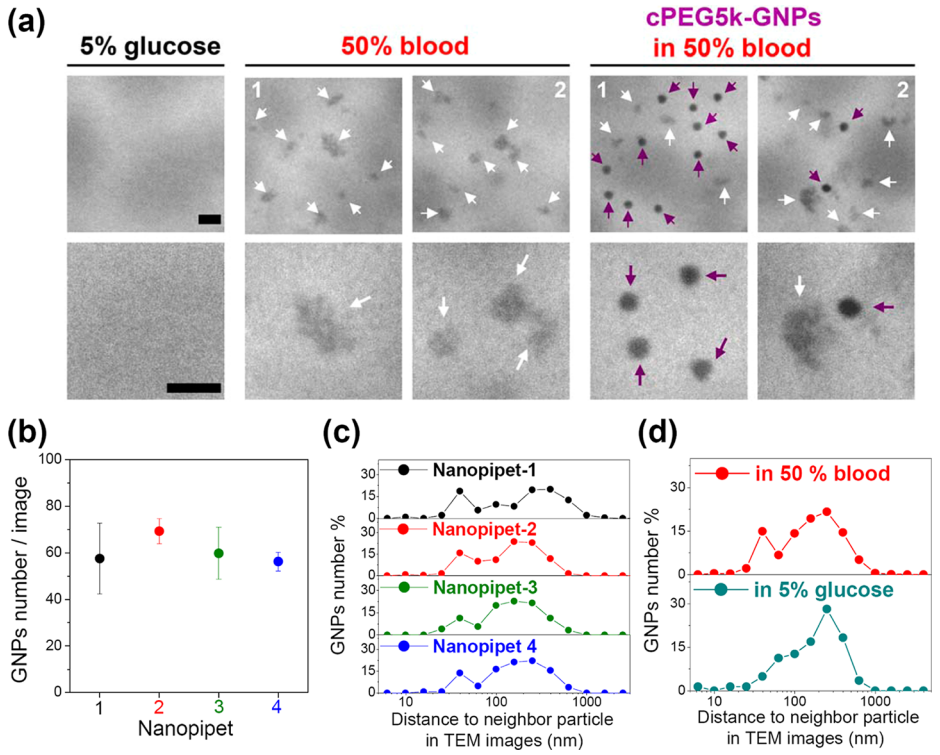

Figure 3. Observation of cPEG5k-GNPs in 50% diluted blood using the TEM nanopipet: (a) TEM images of the 5% glucose solution, the 50% diluted blood, and the cPEG5k-GNPs in the 50% diluted blood in the nanopipets; (b) particle number in the four nanopipets in the TEM image zones (2.0 μm × 2.7 μm); (c) particle number percentage vs the distance to the neighboring particles in the four repeated blood samples in the nanopipets; (d) comparison of the particle number percentage vs distance to neighboring particles for the cPEG5k-GNPs in 50% blood and in 5% glucose. Scale bar is 20 nm.

aggregated on the copper grids (carbon film and SiO_x film) (Figure 2S, Supporting Information). The nanopipet clearly offers a simple and convenient sampling device for preserving and quantifying the native aggregation/agglomeration states of the particles, which are free of any artifacts introduced due to the sampling device.

Furthermore, we examined the possibility of the use of a nanopipet with a well-defined chamber width to sort out certain-sized particles from blood, which is an interesting physiological environment for which the observation and characterization of nanoparticles are challenging.[24,25] In addition to preserving the native spatial distribution of the particles, the defined narrow chamber structure of the nanopipet can also act as a prefilter for simple and convenient sorting of nanosized materials, preventing the entry of larger substances found in blood; in this case, the blood cells and platelets can be excluded in the sample loading process (Figure 1b). Thus, only the submicrometer sized particles in blood plasma smaller than the chamber width of the nanopipet were sampled and observed by TEM. A 50% diluted blood sample was studied using this method, and some irregular-shaped nanoscale substances (5−20 nm) were observed that might be serum proteins, such as serum albumin (Figure 3a). When cPEG5k-GNPs were spiked into the 50% diluted blood, both the gold nanoparticles (indicated with the purple arrow) and the presumed blood proteins (indicated with the white arrow) were easily visualized, recognized, and used for image-based quantitative analysis (Figure 3a). Four nanopipets were used to load the particles from the same 50% diluted blood sample, and a similar particle number was observed for each (Figure 3b). The even spatial distribution of the particles and the reproducible quantitative results reveal that the nanopipet is a promising sampling device for sorting particles from blood. Moreover, the aggregation/agglomeration states of the cPEG5k-GNPs in the 50% diluted blood were evaluated by plotting the particle number percentage vs the distance to the neighboring particles (d). In Figure 3c, four repeated trials showed that the cPEG5k-GNPs exhibited a broad peak (~80% particles) with distances to the neighbor particles that were larger than the diameter of the cPEG5k-GNPs, indicating that most of the particles were well dispersed in the blood. A small additional peak appearing near the diameter of the cPEG5k-GNPs (~39.6 nm) with particle number percentages of 21.7%, 18.4%, 15.4%, and 15.6% was also observed for all four of the repeated nanopipets. Because only a single peak was observed when the same concentration of cPEG5k-GNPs was spiked into a 5% glucose solution, the additional aggregation peak with a particle number of ~18% reveals that the 50% diluted blood induces a slight aggregation of the particles (Figure 3d). The results confirm that the nanopipet offers a simple and convenient sampling device for sorting nanoparticles and estimating the aggregation/agglomeration states of nanoparticles in blood with reproducible and quantitative results and can also be used for the anlaysis of other biological fluids of interest. Moreover, intentionally aggregated, citrate-modified gold nanoparticles (citrate-GNPs) were examined. In 5% glucose, the citrate-GNPs showed ~70% aggregation with 2−10 nanoparticles in each aggregate, while in 50% diluted blood, the extent of aggregation of the particles increased to ~87%, with ~40% of the aggregates containing 11−100 particles in each aggregate (Figure 3S, Supporting Information). The nanopipet may, therefore, potentially be able

dx.doi.org/10.1021/ac301523n | *Anal. Chem.* 2012, 84, 6312−6316

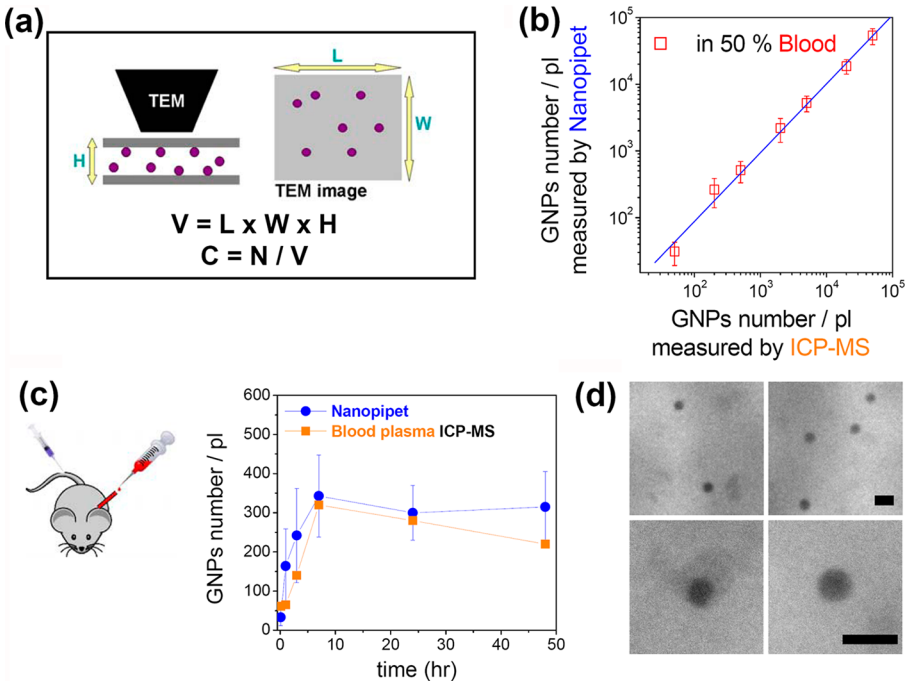

Figure 4. Quantification of the cPEG5k-GNP concentration in blood samples using the TEM nanopipet and ICPMS analyses: (a) concept for quantifying the concentration of nanoparticles using the nanopipet; (b) determination of the cPEG5k-GNPs concentration in 50% diluted blood using ICPMS and a nanopipet (n = 3). The blue line is the linear fitting result with a slope = 1.03 (C_{ICPMS} = $C_{nanopipet}$) and r^2 = 0.997. (c) Determination of the cPEG5k-GNPs concentration in whole blood samples from a single rat at t = 0.1, 1, 3, 7, 24, and 48 h using ICPMS (n = 1) and the nanopipet (n = 3) analytical methods. No significant difference was found between the two methods using the t test ($p \leq 0.05$) and (d) TEM images of the cPEG5k-GNPs in the whole blood of a rat. Scale bar is 20 nm.

to distinguish the aggregation extent of intentionally aggregated nanoparticles in different aqueous environments.

Quantifying the concentration of nanoparticles in a biological matrix is important for in vivo analysis of their absorption, distribution, metabolism, and excretion, as well as for pharmacokinetic and toxicity studies,[26,27] particularly for nanoparticles composed of elements that are abundant in the biological fluids in the body (e.g., C, H, O, N, P, Fe, Zn, and Ca) yet still remains a common challenge. In addition to preserving the native spatial distribution of the particles in order to prepare a homogeneous specimen and act as a prefilter for sorting particles from blood, the fixed and well-defined narrow-chamber volume of the nanopipet has an image volume (V) equal to the TEM image area multiplied by the chamber width of the nanopipet ($V = L \times W \times H$). The particle number (N) in each TEM image was thus counted and divided by the total imaged volume to determine the particle concentration (C) in each sample solution ($C = N/V$) (Figure 4a). The number of cPEG5k-GNPs in the nanopipet counted in the TEM images was then compared to the ICPMS analysis, which is the gold standard method for quantifying the concentration of metals (such as Au, Ag, Fe, etc.). The particle concentration of the cPEG5k-GNPs counted in the nanopipets (n = 3) and calculated by ICPMS are consistent in the particle concentration range from 5×10^{10} to 5×10^{13} particles/mL in 50% diluted blood (Figure 4b). Furthermore, cPEG5k-GNPs in 5% glucose (400 μL, 3×10^{14} particles/mL) were injected intravenously in a rat, and blood samples were collected following injection (t = 0.1, 1, 3, 7, 24, 48 h). Each whole blood sample was sorted using nanopipets (n = 3) and analyzed by ICPMS. Figure 4c shows the comparable results obtained for the number of cPEG5k-GNPs counted in the nanopipets and measured by ICPMS. This experiment confirmed that the nanopipet is a simple and convenient sampling device for evaluating the concentration of nanoparticles using TEM. The success is attributed to the ultrasmall sample volume required (<1 μL), and this tool may be used to analyze the particle concentration in local body fluids of interest.

In conclusion, we have constructed a microchip-based nanopipet for the preparation of homogeneous specimens and the sorting of nanoparticles from blood. In addition to morphology-based information, a TEM image-based quantitative method was developed for analyzing the shape, size/size distribution, aggregation/agglomeration states, and concentration of particles in aqueous environments of interest. Moreover, this nanopipet is adaptable to all TEM holders, mass producible, disposable, and convenient for sample loading and observation. A comprehensive physiological characterization of PEGylated gold nanoparticles, including their aggregation/agglomeration state and number of particles in a blood sample demonstrates the potential of this nanopipet device for nanoparticle characterization in biological fluids. Because the characterization is based on observation of individual particles, this method can be easily extended to other particle-based materials, particularly for quantifying nanoparticles composed of the elements that are abundant in biological fluids (e.g., C, H, O, N, P, Fe, Zn, and Ca). In addition to observation under dry conditions, the sorted thin layer sample solution may be sealed in nanopipets and imaged in the native aqueous environment.[28−30] In this study, therefore, we demonstrated that our nanopipet, a simple and conventional sampling device, offers the possibility of the use of TEM to quantitatively characterize the size/size distribution, shape, aggregation/agglomeration state, and particle concentration of nanomaterials in various native environments of interest.

dx.doi.org/10.1021/ac301523n | *Anal. Chem.* 2012, 84, 6312−6316

■ ASSOCIATED CONTENT

Supporting Information

Additional information as noted in text. This material is available free of charge via the Internet at http://pubs.acs.org.

■ AUTHOR INFORMATION

Corresponding Author

*C.-S.Y.: tel, 886-37246166 ext 38100; fax, 886-37586447; e-mail, cyang@nhri.org.tw. T.-R.Y.: tel, + 886-936347230; fax, 886-3-5722366; e-mail, tryew@mx.nthu.edu.tw.

Author Contributions

The manuscript was written through contributions of all authors. All authors have given approval to the final version of the manuscript.

Notes

The authors declare no competing financial interest.

■ ACKNOWLEDGMENTS

The authors acknowledge financial support from Taiwan National Health Research Institutes Foundation (Grants NM-099-PP-05 and NM-100-PP-05) and from the Materials Analysis Corporation under the program "Physicochemical Characterization of Nanopharmaceuticals-Transmission Electron Microscopy Based Analysis Platform".

■ REFERENCES

(1) Yoo, J. W.; Irvine, D. J.; Discher, D. E.; Mitragotri, S. *Nat. Rev. Drug Discovery* **2011**, *10*, 521−535.

(2) Geng, Y.; Dalhaimer, P.; Cai, S. S.; Tsai, R.; Tewari, M.; Minko, T.; Discher, D. E. *Nat. Nanotechnol.* **2007**, *2*, 249−255.

(3) Chithrani, B. D.; Ghazani, A. A.; Chan, W. C. W. *Nano Lett.* **2006**, *6*, 662−668.

(4) Lammers, T.; Aime, S.; Hennink, W. E.; Storm, G.; Kiessling, F. *Acc. Chem. Res.* **2011**, *44*, 1029−1038.

(5) Perry, J. L.; Herlihy, K. P.; Napier, M. E.; Desimone, J. M. *Acc. Chem. Res.* **2011**, *44*, 990−998.

(6) Lee, P. Y.; Wong, K. K. Y. *Curr. Drug Delivery* **2011**, *8*, 245−253.

(7) Zamborini, F. P.; Bao, L.; Dasari, R. *Anal. Chem.* **2012**, *84*, 541−576.

(8) Sapsford, K. E.; Tyner, K. M.; Dair, B. J.; Deschamps, J. R.; Medintz, I. L. *Anal. Chem.* **2011**, *83*, 4453−4488.

(9) Sanhai, W. R.; Sakamoto, J. H.; Canady, R.; Ferrari, M. *Nat. Nanotechnol.* **2008**, *3*, 242−244.

(10) Domingos, R. F.; Baalousha, M. A.; Ju-Nam, Y.; Reid, M. M.; Tufenkji, N.; Lead, J. R.; Leppard, G. G.; Wilkinson, K. J. *Environ. Sci. Technol.* **2009**, *43*, 7277−7284.

(11) McCall, M. J. *Nat. Nanotechnol.* **2011**, *6*, 613−614.

(12) Bawa, R. *Curr. Drug Delivery* **2011**, *8*, 227−234.

(13) Bawarski, W. E.; Chidlowsky, E.; Bharali, D. J.; Mousa, S. A. *Nanomed. Nanotechnol. Biol. Med.* **2008**, *4*, 273−282.

(14) Helmus, M. *Nat. Nanotechnol.* **2007**, *2*, 333−334.

(15) Leapman, R. D. *Nat. Nanotechnol.* **2010**, *5*, 480−481.

(16) Lengyel, J. S.; Milne, J. L. S.; Subramaniam, S. *Nanomed.* **2008**, *3*, 125−131.

(17) Sander, B.; Golas, M. M. *Micros. Res. Tech.* **2011**, *74*, 642−663.

(18) Jun, S. M.; Ke, D. X.; Debiec, K.; Zhao, G. P.; Meng, X.; Ambrose, Z.; Gibson, G. A.; Watkins, S. C.; Zhang, P. J. *Structure* **2011**, *19*, 1573−1581.

(19) Deegan, R. D.; Bakajin, O.; Dupont, T. F.; Huber, G.; Nagel, S. R.; Witten, T. A. *Nature* **1997**, *389*, 827−829.

(20) Murphy, C. J.; Gole, A. M.; Stone, J. W.; Sisco, P. N.; Alkilany, A. M.; Goldsmith, E. C.; Baxter, S. C. *Acc. Chem. Res.* **2008**, *41*, 1721−1730.

(21) Diao, J.; Ren, D.; Engstrom, J. R.; Lee, K. H. *Anal. Biochem.* **2005**, *343*, 322−328.

(22) Kutsay, O.; Loginova, O.; Gontar, A.; Perevertallo, V.; Zanevskyy, O.; Katrusha, A.; Ivakhnenko, S.; Gorokhov, V.; Stank, S.; Tkach, V.; Novikov, N. *Diamond Relat. Mater.* **2008**, *17*, 1689−1691.

(23) Sul, O.; Tsai, C. E.; Gao, N.; Yang, E. H. *Nanosci. Nanotechnol. Lett.* **2010**, *2*, 133−138.

(24) Braeckmans, K.; Buyens, K.; Bouquet, W.; Vervaet, C.; Joye, P.; Vos, F. D.; Plawinski, L.; Doeuvre, L. c.; Angles-Cano, E.; Sanders, N. N.; Demeester, J.; Smedt, S. C. D. *Nano Lett.* **2010**, *10*, 4435−4442.

(25) Williams, S. K. R.; Runyon, J. R.; Ashames, A. A. *Anal. Chem.* **2011**, *83*, 634−642.

(26) Xie, H.; Gill-Sharp, K. L.; O'Neal, P. *Nanomed. Nanotechnol. Biol. Med.* **2007**, *3*, 89−94.

(27) Nikitin, M. P.; Torno, M.; Chen, H.; Rosengart, A.; Nikitin, P. I. *J. Appl. Phys.* **2008**, *103*, 07A304−07A304−3.

(28) de Jonge, N.; Ross, F. M. *Nat. Nanotechnol.* **2011**, *6*, 695−704.

(29) Liu, K. L.; Wu, C. C.; Huang, Y. J.; Peng, H. L.; Chang, H. Y.; Chang, P.; Hsu, L.; Yew, T. R. *Lab Chip* **2008**, *8*, 1915−1921.

(30) Grogan, J. M.; Bau, H. H. *J. Microelectromech. Syst.* **2010**, *19*, 885−894.